

Gravitational waves and rotational properties of hypermassive neutron stars from binary mergers

*21st International Conference on General Relativity and Gravitation
Columbia University, New York, 11. July 2016*

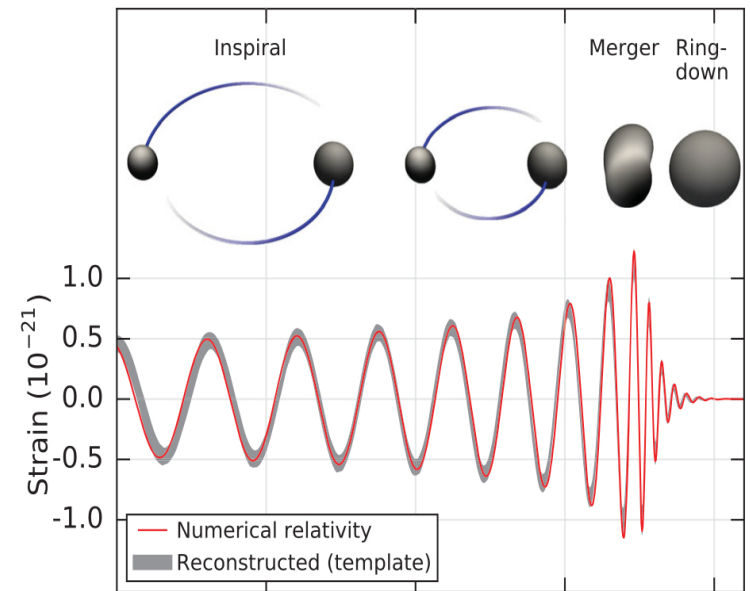
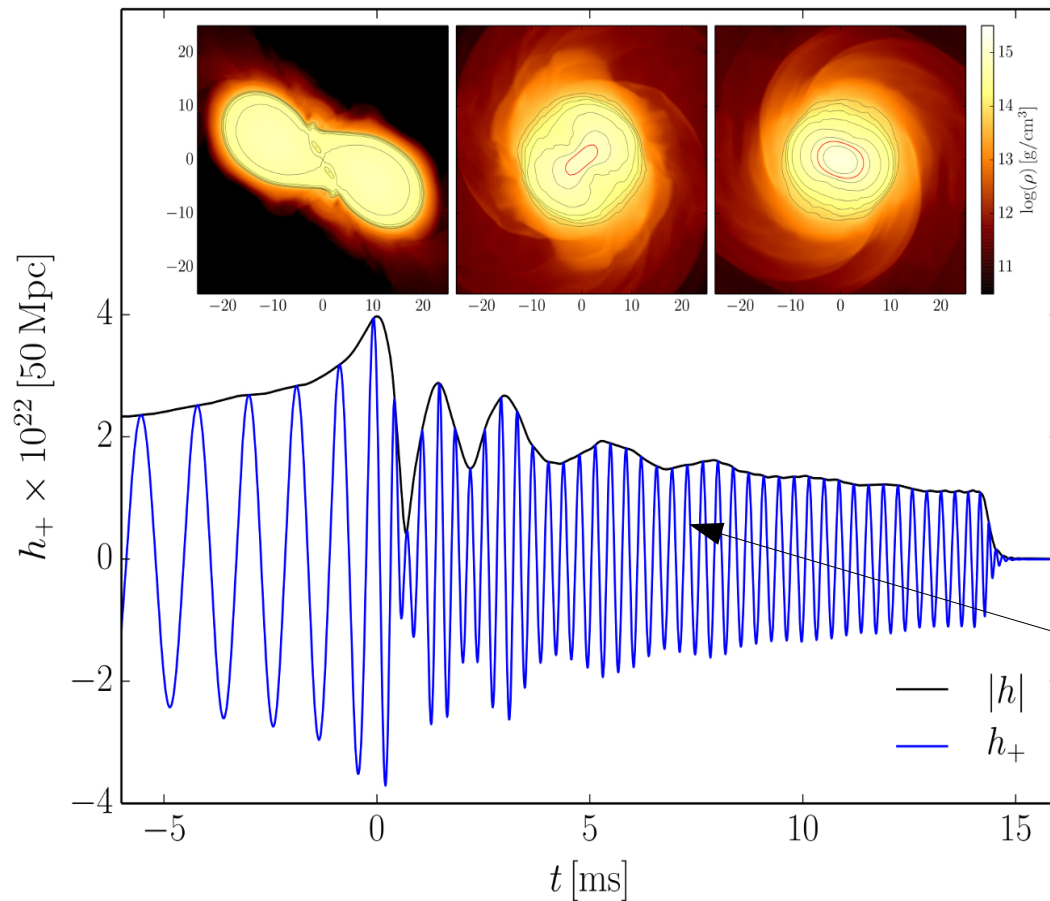
*Matthias Hanauske, Kentaro Takami, Luciano Rezzolla, Filippo Galeazzi,
José A. Font, Bruno Mundim, Luke Bovard, and Horst Stöcker*

*Frankfurt Institute for Advanced Studies
Johann Wolfgang Goethe-University
Institute for Theoretical Physics
Department of Relativistic Astrophysics
Frankfurt am Main, Germany*

Gravitational Waves from Binary Neutron Star Mergers

Neutron star merger (Simulation)

Merger of two Black Holes



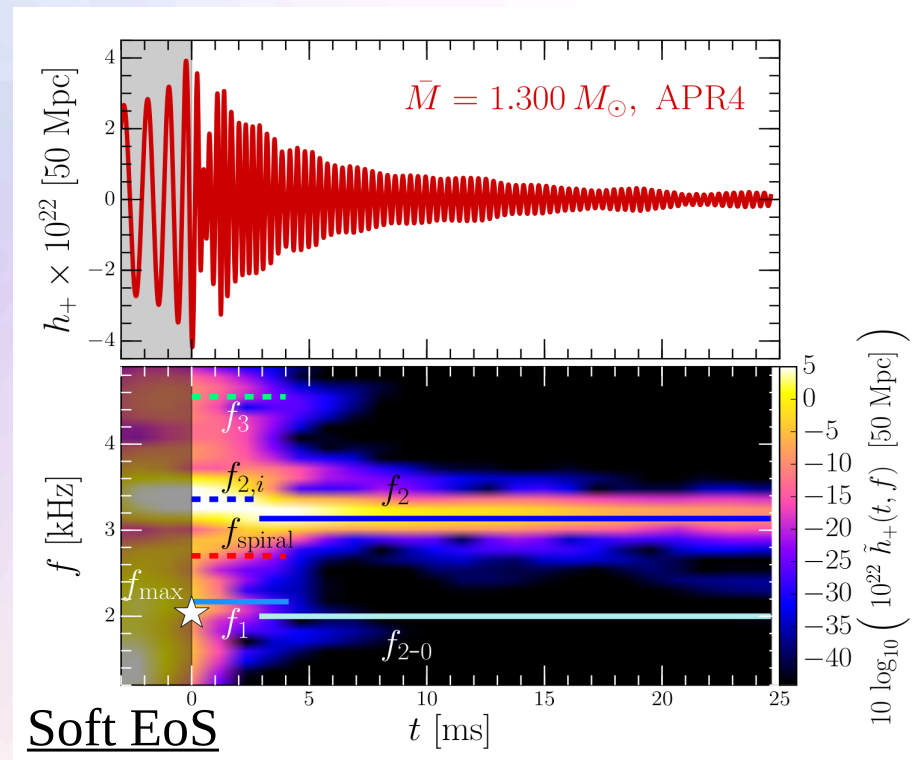
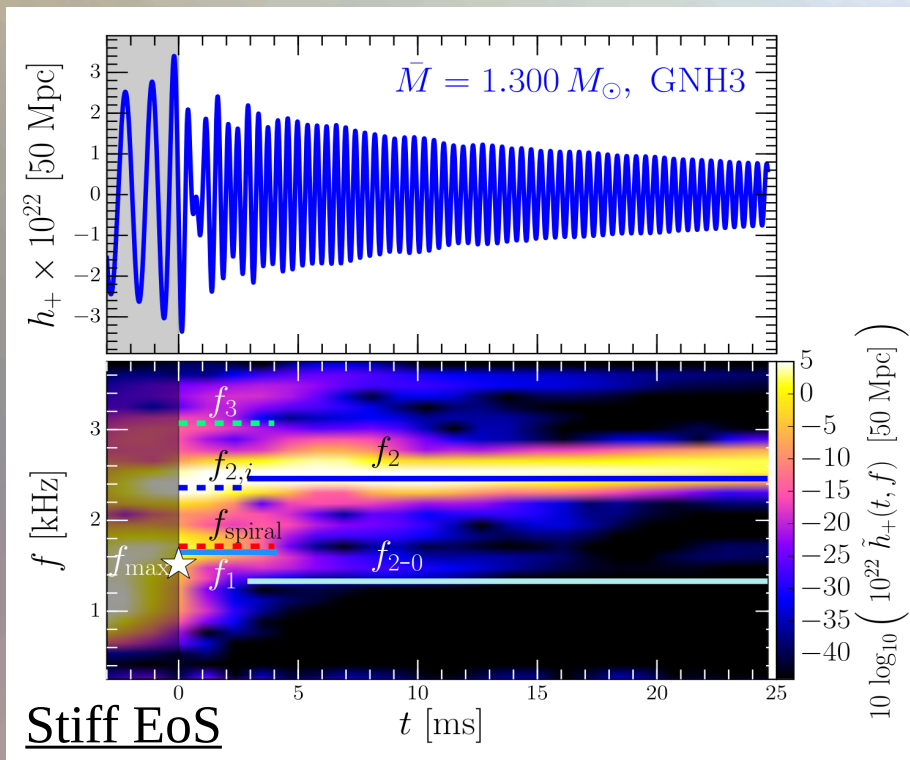
Main Difference:
Neutron star mergers could have a
post-merger phase

Time Evolution of the GW-Spectrum depends on the Equation of State

Early post-merger emission: frequencies f_{\max} , f_1 , f_2 , f_3 and f_{2-0}

$t > 5$ ms after merger: dominant frequency is the f_2 -frequency

See L.Rezzolla and K.Takami, arXiv:1604.00246



Evolution of the frequency spectrum of the emitted gravitational waves for the stiff GNH3 (left) and soft APR4 (right) EOS.

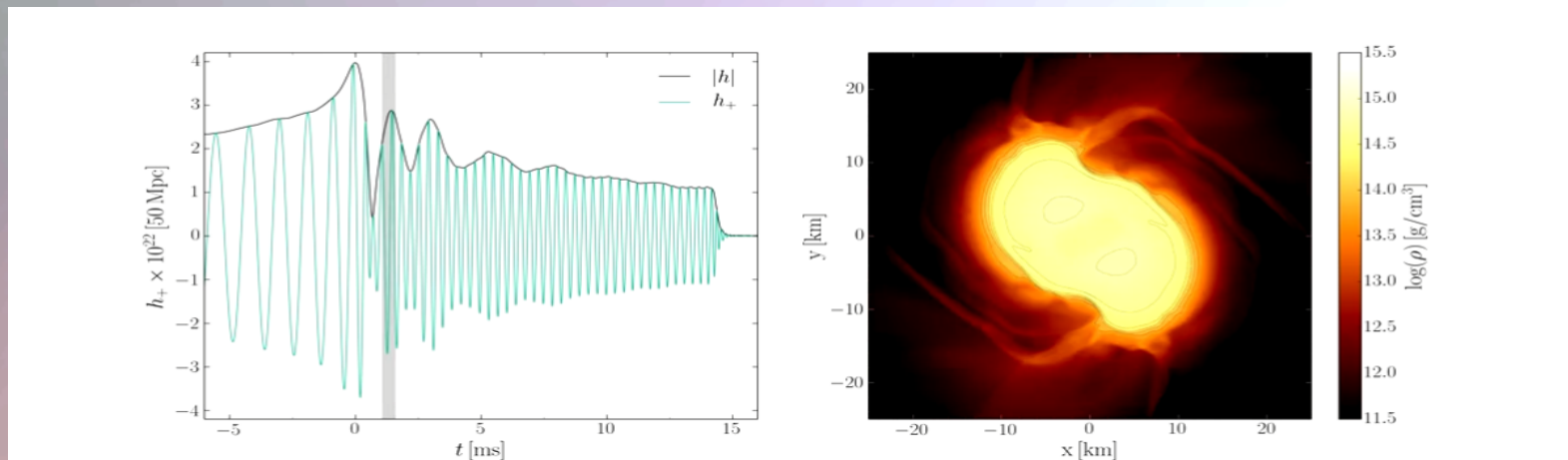
Numerical Setup

Several different EOSs : ALF2, APR4, GNH3, H4 and Sly, approximated by piecewise polytopes. Thermal ideal fluid component ($\Gamma=2$) added to the nuclear-physics EOSs.

Grid Structure:

Adaptive mesh refinement (six ref. levels)
Grid resolution: (from 221 m to 7.1 km)
Initial separation of stellar cores: 45 km

BSSNOK conformal traceless formulation of the ADM equations. 3+1 Valencia formulation and high resolution shock capturing methods for the hydrodynamic evolution. Full general relativity using the **Einstein-Toolkit** and the **WHISKY/WhiskyTHC code** for the general-relativistic hydrodynamic equations.



The Angular Velocity in the (3+1)-Split

The angular velocity Ω in the (3+1)-Split is a combination of the lapse function α , the ϕ -component of the shift vector β^ϕ and the 3-velocity v^ϕ of the fluid (spatial projection of the 4-velocity \mathbf{u}):

$$\Omega(x, y, z, t) = \frac{u^\phi}{u^t} = \alpha v^\phi - \beta^\phi$$

Angular
velocity Ω

Lapse function
 α

Φ -component
of 3-velocity v^ϕ

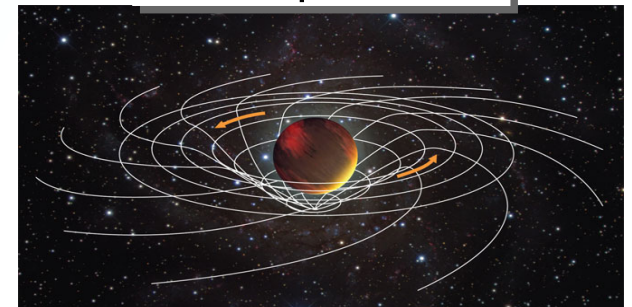
(3+1)-decomposition
of spacetime:

$$g_{\mu\nu} = \begin{pmatrix} -\alpha^2 + \beta_i \beta^i & \beta_i \\ \beta_i & \gamma_{ij} \end{pmatrix}$$

Frame-dragging
 β^ϕ

Focus: Inner core of the differentially rotating HMNS

- M. Shibata, K. Taniguchi, and K. Uryu, Phys. Rev. D 71, 084021 (2005)
- M. Shibata and K. Taniguchi, Phys. Rev. D 73, 064027 (2006)
- F. Galeazzi, S. Yoshida and Y. Eriguchi, A&A 541, p. A156 (2012)
- W. Kastaun and F. Galeazzi, Phys. Rev. D 91, p. 064027 (2015)



Rotation Profiles (ALF2-1.35 Model)

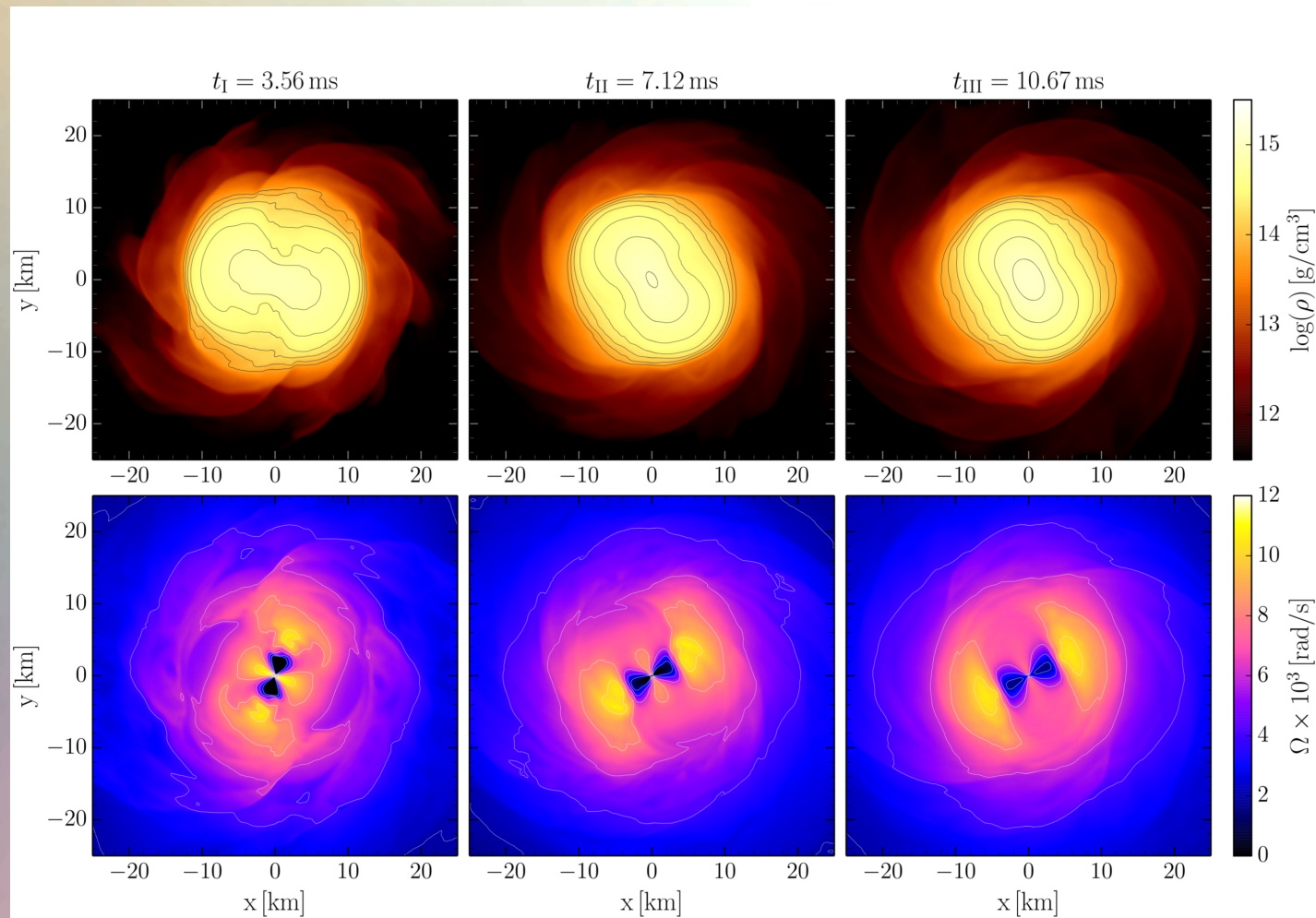


FIG. 3. Logarithm of the rest mass density $\text{Log}(\rho)$ [g/cm³] (upper row) and fluid angular velocity $\Omega \times 10^3$ [rad/s] (lower row) in the xy -plane for the ALF2-M135 model at three different post-merger times. The iso-contour curves have been drawn at $13.8 + 0.2n$ (upper row) and $2n$ (lower row), $n \in \mathbb{N}$.

Rotation Profiles (ALF2-1.25 Model)

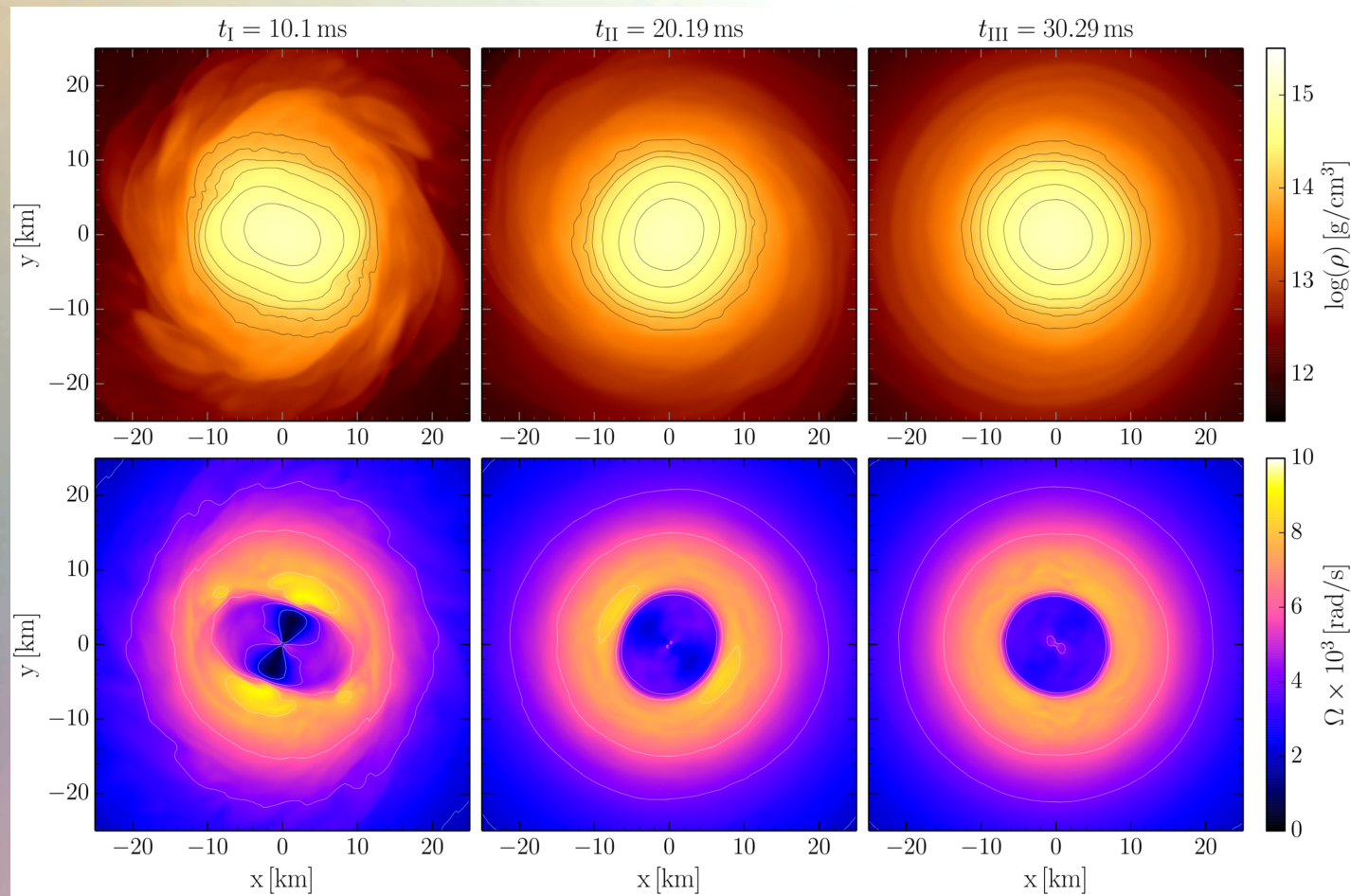


FIG. 11. Logarithm of the rest mass density $\log(\rho)$ [g/cm³] (upper row) and fluid angular velocity $\Omega \times 10^3$ [rad/s] (lower row) in the xy -plane for the ALF2-M125 model at three different post-merger times. The iso-contour curves have been drawn at $13.8 + 0.2n$ (upper row) and $2n$ (lower row), $n \in \mathbb{N}$

Frame-Dragging and Gravitomagnetism

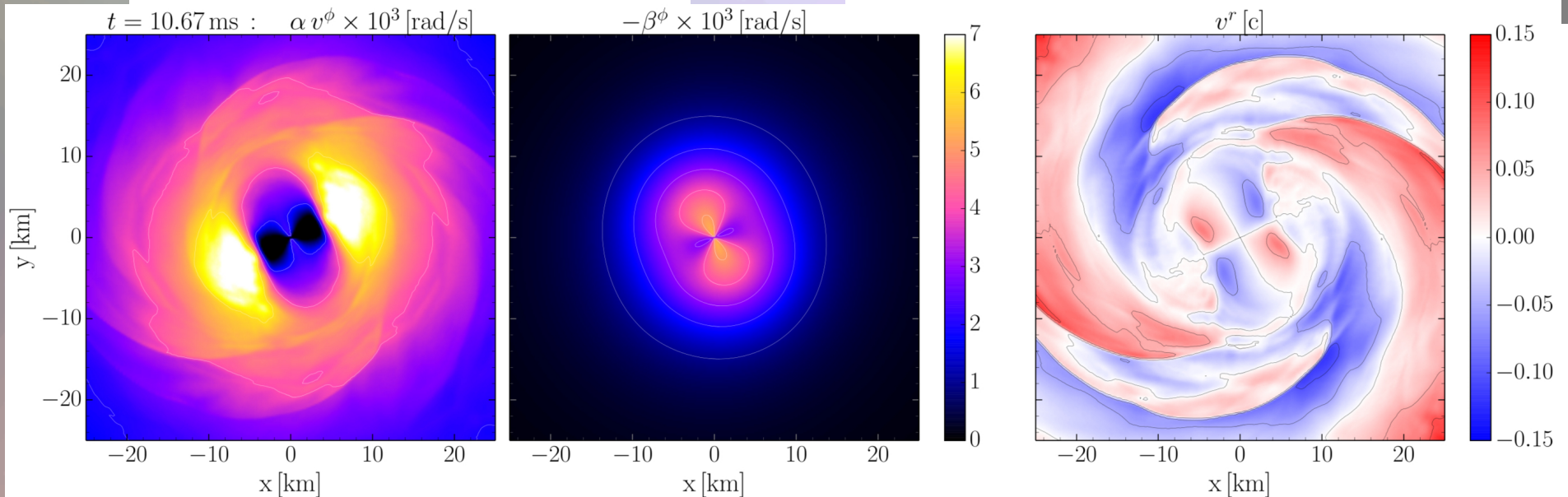
The dragging of local inertial frames is quite large in the interior of the HMNS and therefore an additional gravitomagnetic force is present. Like the Lorentz-force in electromagnetism, it acts orthogonal to the fluids velocity and the frame dragging.

Ingredients of the angular velocity:

$$\Omega(x, y, z, t) = \frac{u^\phi}{u^t} = \alpha v^\phi - \beta^\phi$$

$$\frac{d\mathbf{v}}{d\tau} = -\text{grad } \Phi(\mathbf{r}) + 2\boldsymbol{\Omega}^F(\mathbf{r}) \times \mathbf{v} + \mathcal{O}(v^2/c^2), \quad (11)$$

(strong time and
 ϕ -dependence !)



The Gravitomagnetic Effect in the Interior of the HMNS at Medium Post-Merger Times ($4 \text{ ms} < t < 15 \text{ ms}$)

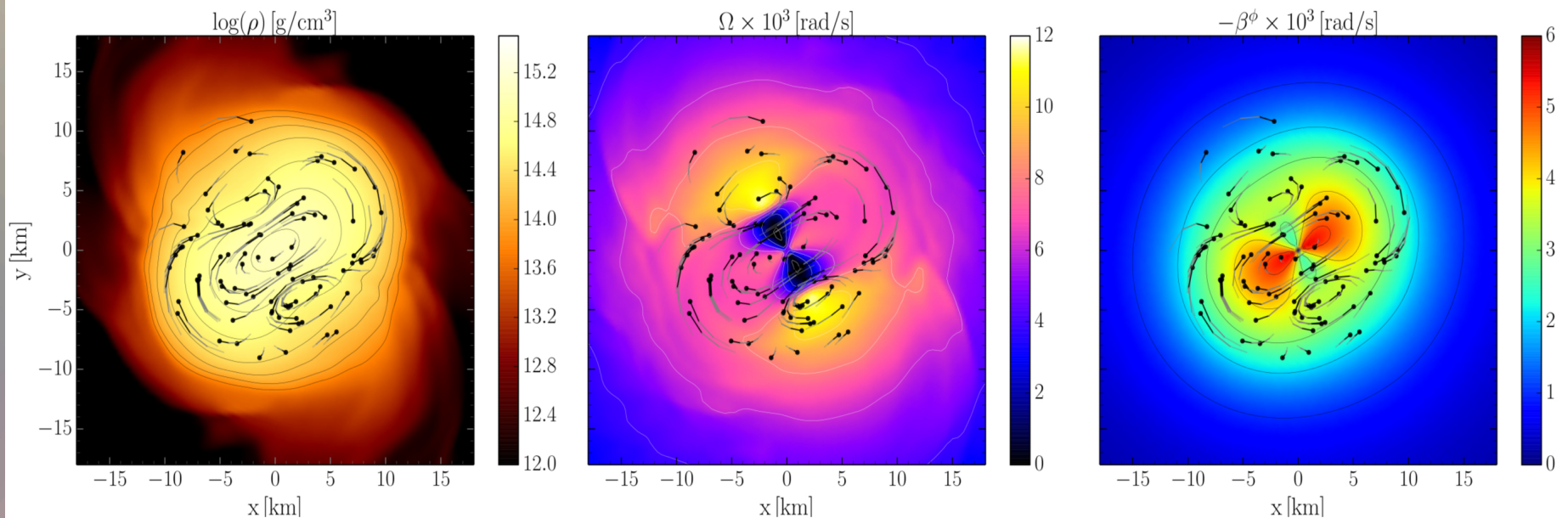


FIG. 7. Logarithm of the rest mass density $\text{Log}(\rho)$ [g/cm³] (left picture), the fluid angular velocity $\Omega \times 10^3$ [rad/s] (middle) and $-\beta^\phi \times 10^3$ [rad/s] (right picture) in the xy-plane for the SLY-M132 model at $t = 6.71 \text{ ms}$. The trajectories of several tracer-cells are additionally mapped for two previous times (separation $\Delta t_{Tr} = 0.095 \text{ ms}$).

The Interior of the HMNS at Late Post-Merger Times ($t > 15$ ms)

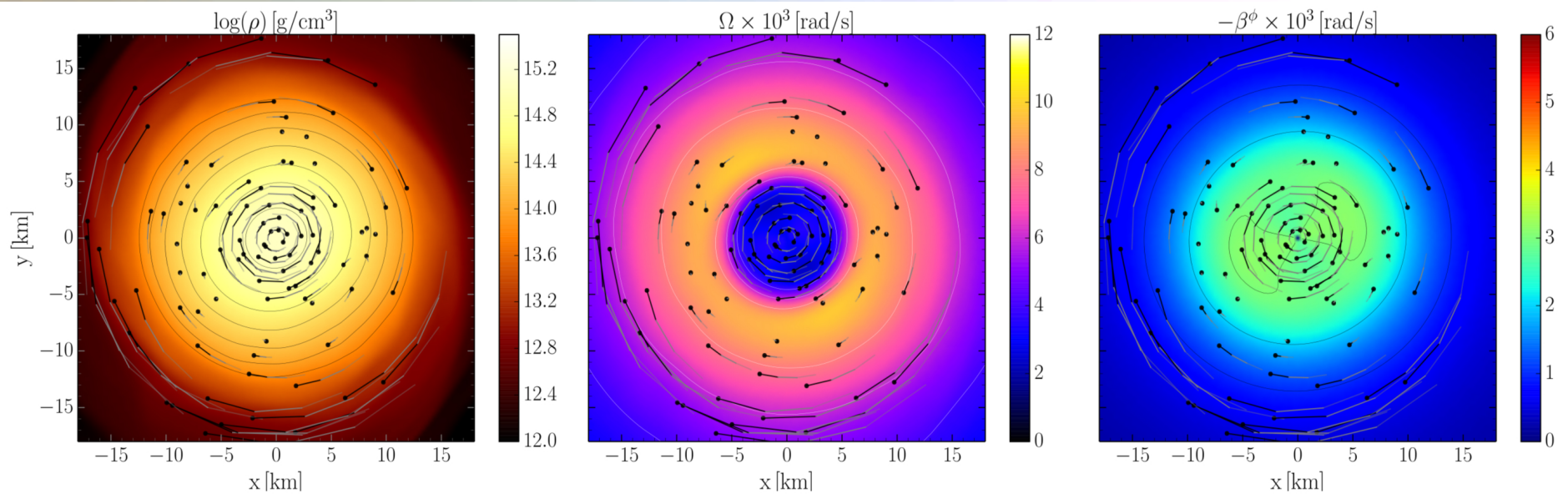
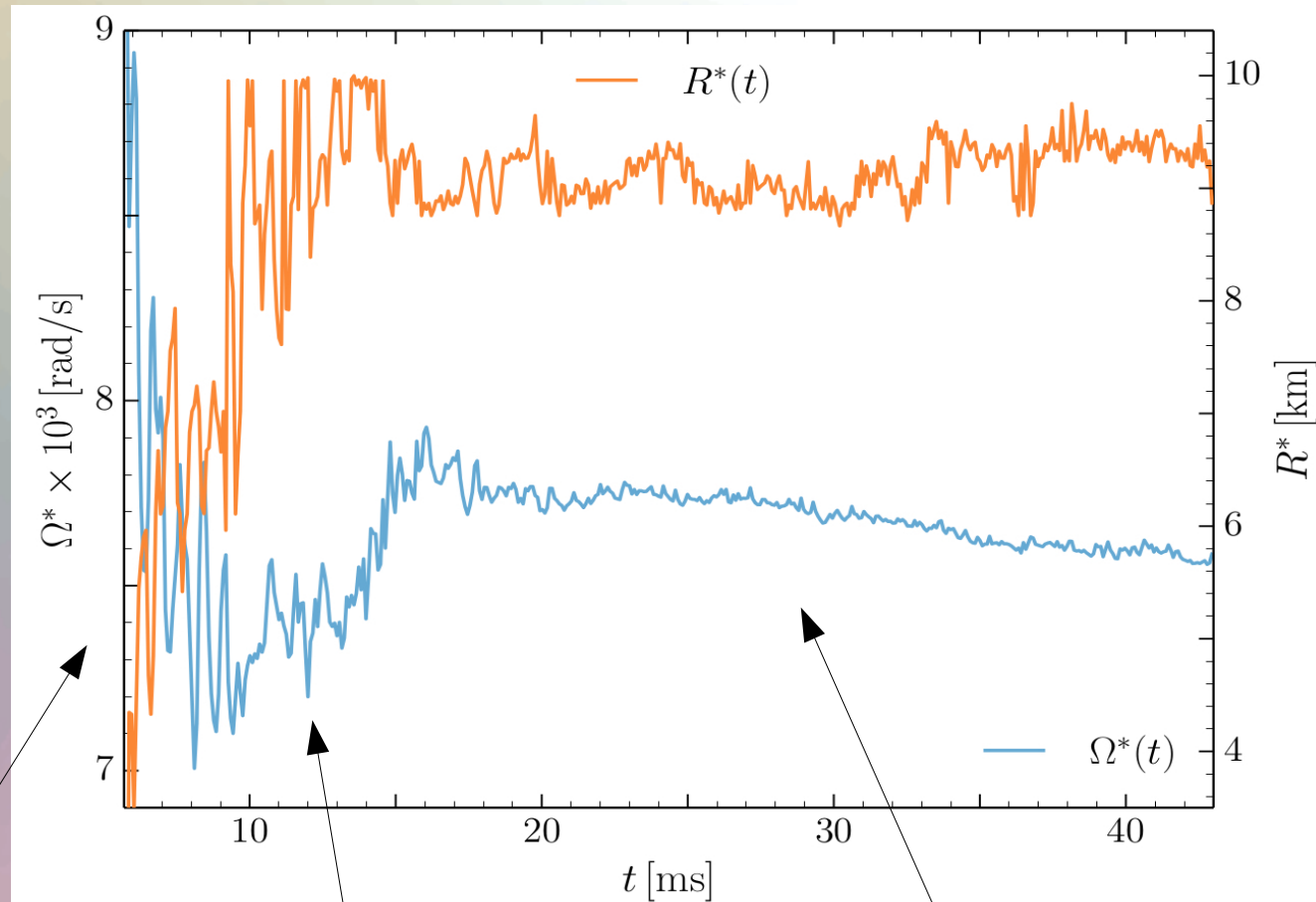


FIG. 8. Same as in Fig. 7, but at $t = 23.83$ ms.

Maximum Value of Ω and its Radial Position



$t < 5$ ms
Violent early phase

$5 \text{ ms} < t < 15$ ms
Gravitomagnetism

$t > 15$ ms:
Quasi equilibrated and ϕ -symmetric HMNS

Averaging Procedure for Ω

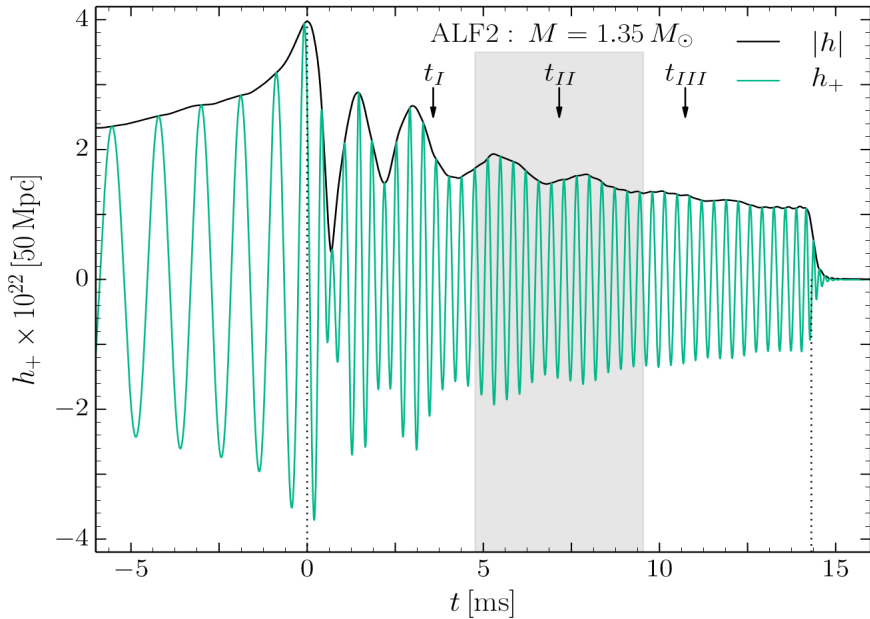


FIG. 2. Gravitational wave amplitude $|h|$ and h_+ at a distance of 50 Mpc for the ALF2-M135 model.

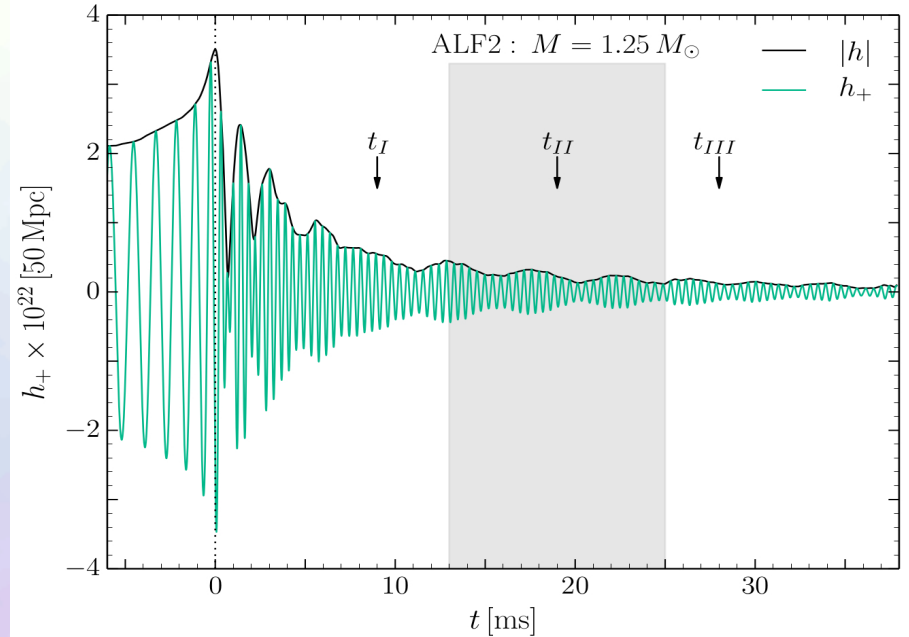
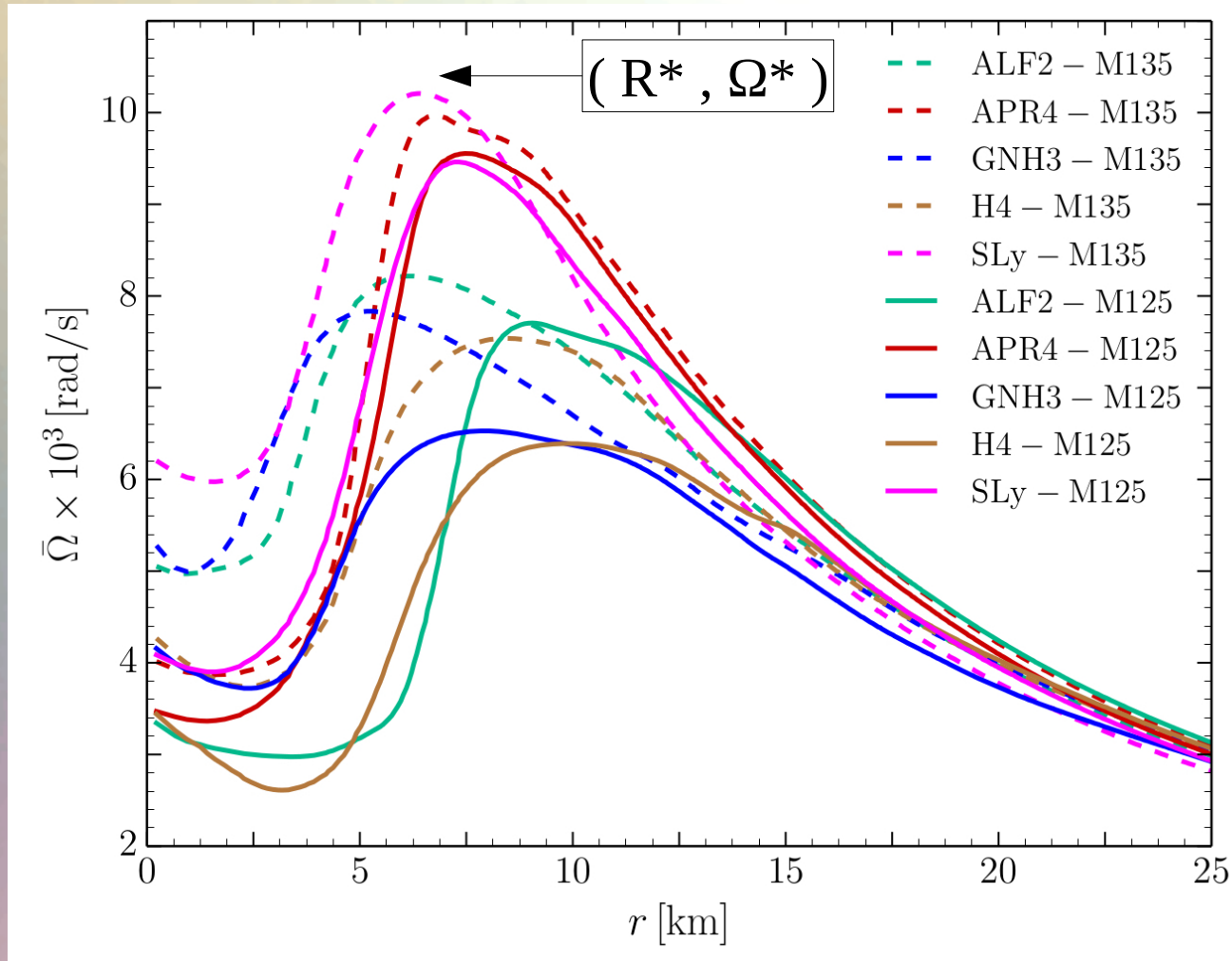


FIG. 10. Gravitational wave amplitude h_+ and $|h|$ at a distance of 50 Mpc for the ALF2-M125 model.

In order to compare the structure of the rotation profiles between the different EOSs, a certain time averaging procedure has been used:

$$\bar{\Omega}(r, t_c) = \int_{t_c - \Delta t/2}^{t_c + \Delta t/2} \int_{-\pi}^{\pi} \Omega(r, \phi, t') d\phi dt'$$

Time-averaged Rotation Profiles



Time-averaged rotation profiles for different EoS
Low mass runs (solid curves), high mass runs (dashed curves).

Gravitational Waves and the maximum of the Rotation Curve

